Journal of Sensor Science and Technology
Vol. 34, No. 1 (2025) pp. 55-62
http://dx.doi.org/10.46670/JSST.2025.34.1.55
pISSN 1225-5475/eISSN 2093-7563

Study on Orthogonal Fluxgate Sensor with High Sensitivity and Wide Dynamic Range for Magnetic Flux Leakage Testing

Sangyeol Kim[1], Kyung-won Kim[1], and Daesung Lee[1,+]

Abstract

Magnetic flux leakage (MFL) detection testing is a widely used inspection method for detecting pipeline defects by sensing the magnetic flux leaked from defects. Various magnetic sensors have been studied for applications in MFL detection testing, with Hall sensors being the most commonly used because of their wide dynamic ranges. However, owing to their low sensitivity, Hall sensors exhibit limitations in detecting small defects. We developed an orthogonal fluxgate (OFG) sensor that maintains an appropriate dynamic range for an MFL magnetic environment while achieving high sensitivity. The OFG sensor consists of an excitation coil with an Fe-based amorphous ribbon core and a pickup coil that detects the output voltage induced by the excitation coil. We determined the sensitivity and dynamic range of the sensor by optimizing the shape of the core, which is influenced by shape anisotropy. By adjusting the OFG sensor core length (2 mm, 4 mm, 6 mm) and thickness (50 μm, 150 μm), we confirmed a tradeoff between sensitivity and dynamic range. As a result, we developed an OFG sensor with a dynamic range of ±3 mT and a high sensitivity of 3,130 V/T. Furthermore, the application of the OFG sensor in MFL detection testing successfully detected defects and confirmed its suitability for such applications.

Keywords: Magnetic flux leakage, Magnetic sensor, Orthogonal fluxgate, Sensitivity, Dynamic range

1. INTRODUCTION

Pipeline transportation is essential to ensure a stable supply of oil and natural gas. However, the formation of defects in pipelines can result in substantial economic losses and lead to severe consequences such as environmental contamination and safety incidents [1]. Consequently, regular monitoring of pipeline conditions is imperative. Early detection of defects and the formulation of maintenance plans are essential [2].

Nondestructive testing (NDT) techniques are essential for evaluating pipeline conditions and offer the significant advantage of detecting defects without damaging or disassembling pipeline structures [3]. Among the various NDT methodologies, magnetic flux leakage (MFL) detection testing is widely used for pipeline defect detection. MFL detection testing involves the magnetization of a ferromagnetic pipe and subsequent detection of changes in the magnetic field that leaks from pipe defects. This technology enables rapid and efficient inspection of large-scale structures and serves as a standard inspection method in various industrial sectors including oil and gas pipelines [4].

Currently, Hall sensors are the most commonly used sensors for MFL detection testing. Hall sensors have been widely adopted because of their cost-effectiveness and wide dynamic ranges. However, their low sensitivity limits their ability to detect minor magnetic field variations caused by defects. These limitations increase the risk of unexpected accidents during extended pipeline operation. Therefore, the development of extremely sensitive magnetic sensors is required for precise defect detection [5].

In this study, we aimed to develop an orthogonal fluxgate (OFG) sensor as a high-sensitivity alternative to existing Hall sensors and address the sensitivity limitations of Hall sensors. The OFG sensor demonstrates a tradeoff between sensitivity and dynamic range, which depends on the shape of the magnetic core. By optimizing the design of the OFG sensor, a dynamic range suitable for an MFL testing environment can be achieved. Additionally, we propose the development of an optimized OFG sensor capable of detecting defects with significantly higher sensitivity than that of conventional Hall sensors.

The remainder of this paper is organized as follows. Chapter 2 presents the measurement of the magnetic field levels in an MFL

[1]Smart Sensor Research Center, Korea Electronics Technology Institute
25 Saenari Road, Bundang-gu, Seongnam-si, Gyeonggi-do, Republic of Korea
[+]Corresponding author: leeds@keti.re.kr
(Received: Dec. 20, 2024, Revised: Jan. 3, 2025, Accepted: Jan. 19, 2025)

magnetic environment. Chapter 3 details the design of a high-sensitivity OFG sensor with a dynamic range suitable for measuring magnetic field levels. Chapter 4 analyzes the properties of the optimized OFG sensor and the results obtained from the MFL detection testing. Finally, Section 5 presents the conclusions of this study.

2. MFL MAGNETIC ENVIRONMENT

2.1 MFL Detector Lab Test Version

MFL detection testing is based on applying a DC magnetic field to a pipe and measuring the magnetic flux that leaks from defects. By accurately measuring the magnetic field levels required in the MFL magnetic environment, the sensor's dynamic range can be defined, and the sensor can be optimized accordingly.

In this study, an MFL detector lab test version was constructed based on the laboratory environment shown in Fig. 1. The system consists of an electromagnet, test pipe, and sensor module. The electromagnet and sensor module were fixed, and a test pipe was passed through for the detection of defects.

Fig. 2 shows a simplified model of the MFL detector lab test version structure with and without defects. It consists of an electromagnet, magnetic sensor, and pipe. A direct current was applied to the electromagnet to magnetize the pipe, and the Hall sensor measured the leaked magnetic field.

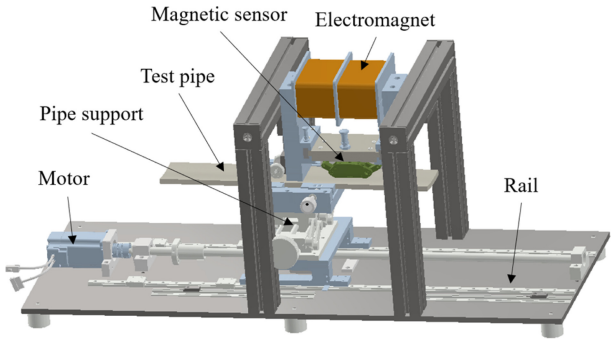

Fig. 1. Structure of MFL detector lab test version

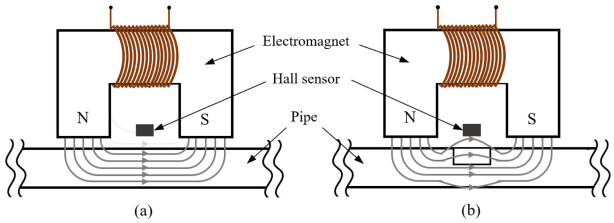

Fig. 2. Principle of MFL sensor : (a) without defect and (b) with defect

As shown in Fig. 2 (a), when no defects were present in the pipe, the magnetized magnetic flux flowed uniformly inside the pipe. At this point, a small offset in the magnetic flux leaks near the pipe surface. This magnetic offset can be used as a baseline to represent the magnetic field level of the desired MFL magnetic environment. As shown in Fig. 2 (b), when a defect exists in the pipe, the magnitude of the leaked magnetic field increases and provides defect detection through the amplitude change in the leaked magnetic field between the baseline and the defect.

2.2 MFL Magnetic Level

Using the constructed MFL detector lab test version, we applied a magnetic field to the pipe and measured the magnetic field leakage. The defects in the test pipes consisted of internal and external defects at depths of 50% and 10% of the pipe thickness. Fig. 3 shows the changes in the magnetic field leakage over time after using an electromagnet to apply a DC magnetic field of 0–25 mT to each test pipe. At this time, the TMAG5170 Hall sensor was applied to the MFL detector lab test version to acquire data via SPI communication.

Fig. 4 (a) shows the amplitude of the magnetic field caused by the defects according to the DC magnetic field intensity applied inside the pipe. The amplitude is the difference between the leaked magnetic field of the baseline and that of the defects. This value represents the actual signal strength and is directly related to defect detection. We confirmed that defects could be detected by applying a magnetic field of 5 mT or higher, as the leaked magnetic field increased with an increase in the magnetic field intensity above 5 mT.

Additionally, applying a sufficient magnetic field of 15 mT or higher ensured more reliable defect signals. Fig. 4 (b) shows the magnetic field that leaked from the pipe as the DC magnetic field intensity applied inside the pipe increased linearly with an increase in the DC magnetic field intensity regardless of the defect type. The stronger the applied DC magnetic field, the larger the leaked magnetic field, which means that higher magnetic field intensities facilitate defect detection.

Through this analysis, we determined the magnetic field levels required for MFL detection testing. We confirmed that applying a strong DC magnetic field of 15 mT or higher provided accurate defect detection. When a DC magnetic field intensity of 15 mT was applied to the pipe, the leaked magnetic field was 3 mT. This study aimed to optimize an OFG sensor with a dynamic range of 3 mT and high sensitivity.

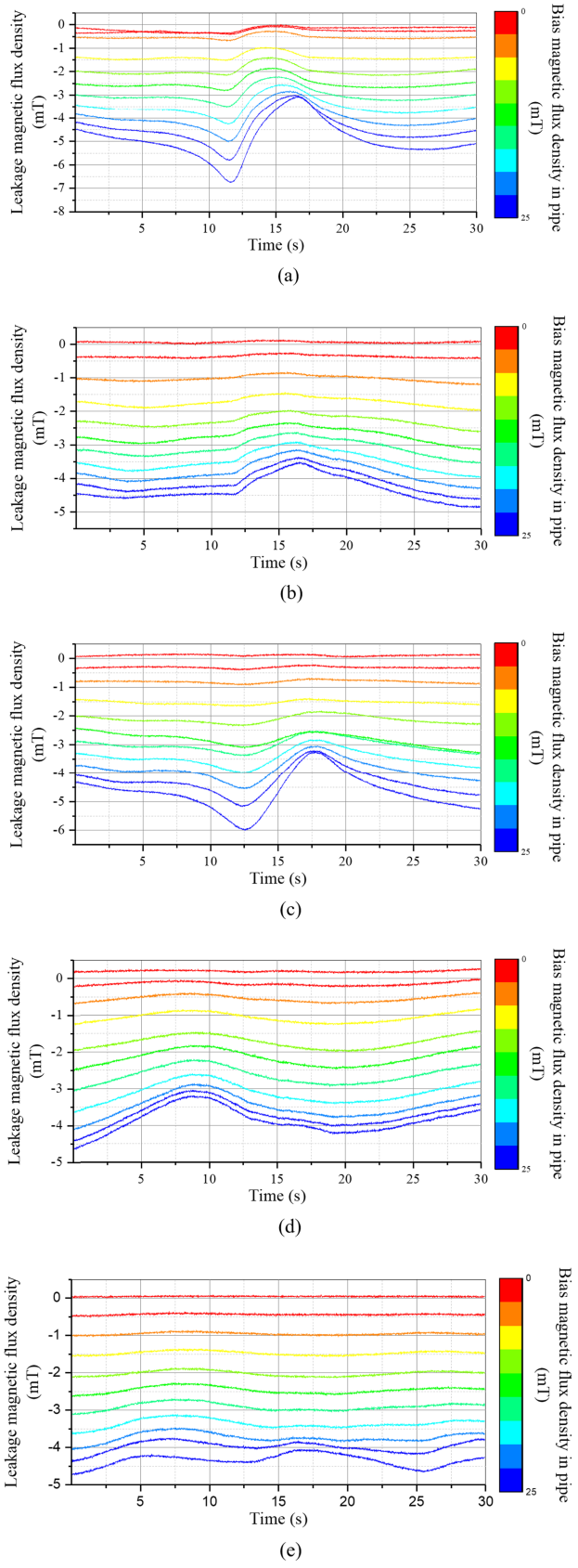

Fig. 3. Measurement results of MFL detector using hall sensor: (a) 50% internal, (b) 10% internal, (c) 50% external, (d) 10% internal, and (e) no defect

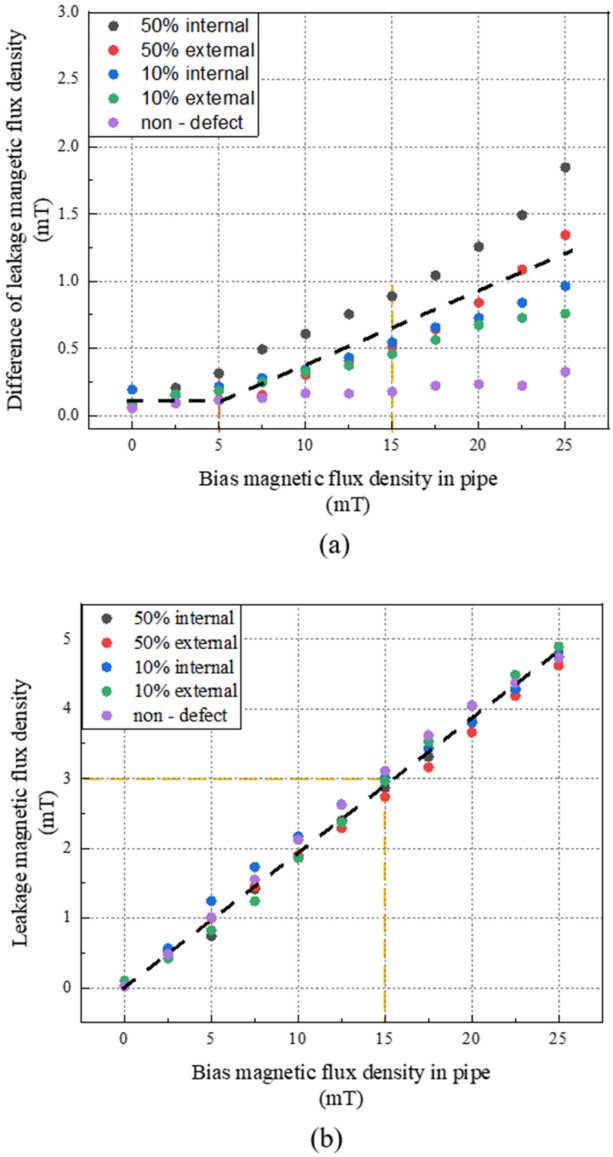

Fig. 4. Analysis graph of MFL detection testing results : (a) MFL magnetic level and (b) difference of leakage magnetic flux density

3. SENSOR DESIGN

3.1 Structure and Operating Principle of OFG sensor

The OFG sensor consists of a ferromagnetic core, excitation coil, and pickup coil as shown in Fig. 5. The ferromagnetic core is a key component that determines the sensitivity of the sensor by reacting sensitively to external magnetic fields.

When an alternating current $I_{ex}(t)$ flows through the excitation coil, a time-varying magnetic field $H_{\varnothing}(t)$ is generated around the core. This magnetic field periodically fluctuates in the Φ-direction

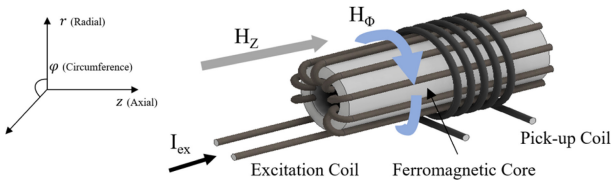

Fig. 5. Structure of OFG sensor

of the core, and according to one of Maxwell's equations,

$$B = \mu H(t)\,, \tag{1}$$

it induces the magnetic flux density B within the core.

When an external magnetic field in the z-direction perpendicular to the excitation is detected, the rotation of the magnetization induces a voltage in the pickup coil. This configuration is termed "orthogonal" because the direction of the core's magnetization and the detection direction are orthogonal to each other.

The OFG sensor output equation

$$V_{out} = -NA\mu_0 H \frac{1-N_d}{[1+N_d(\mu_r-1)]^2}\frac{d\mu_r(t)}{dt} \tag{2}$$

highlights the critical role of the core's relative permeability $\mu_r(t)$ and demagnetizing factor(N_d) in determining the sensor's sensitivity and dynamic range. The relative permeability $\mu_r(t)$ dynamically changes during the magnetization and demagnetization process driven by the excitation coil's alternating current. This change directly influences the sensor output, as a higher rate of permeability variation, ($\frac{d\mu_r(t)}{dt}$, generates a stronger voltage signal in the pickup coil. The demagnetizing factor, N_d, which is determined by the geometry of the core (length and thickness), modulates the internal magnetic field distribution, controls the efficiency of the core magnetization, and reaches saturation.

The sensitivity and dynamic range of the OFG sensor were determined by the number of turns in the pickup coil and the thickness, permeability, and shape of the ferromagnetic core.

3.2 Optimization of OFG Sensor

The OFG sensor core shape is a critical factor determining its sensitivity and dynamic range. Specifically, the core length and thickness significantly influence the permeability changes, saturation characteristics, and shape anisotropy during magnetization–demagnetization. The permeability of the magnetic core is a key parameter that determines the ease of formation and maintenance of magnetization within the core when an external magnetic field is applied.

To optimize the sensor performance, we selected the following core dimensions to systematically explore their effects on sensitivity and dynamic range: core lengths of 2 mm, 4 mm, and 6 mm, and core thicknesses of 50 μm and 150 μm. The core length significantly affects the effective magnetization path; shorter cores reduce the demagnetizing effects and delay saturation, leading to a wider dynamic range but lower sensitivity. Conversely, longer cores exhibit higher sensitivity owing to faster saturation but at the cost of a narrower dynamic range. The core thickness affects the internal magnetic flux density; thinner cores concentrate the magnetic flux and enhance the sensitivity, whereas thicker cores distribute the flux more evenly, thereby increasing the dynamic range. We chose these dimensions carefully to provide a comprehensive analysis of the tradeoff between sensitivity and dynamic range, enabling the optimization of the OFG sensor for applications in MFL testing.

As the core length increases, the overall magnetization path increases. Consequently, maintaining a uniform magnetization state within the core is difficult, which makes it more prone to saturation. Reaching the saturation region more quickly increases the sensitivity. However, once saturation is achieved, the permeability decreases sharply, resulting in a non-linear response to external magnetic fields and a narrowing of the dynamic range.

At this stage, the shape of the core facilitates magnetization in the pre-saturation region. According to Maxwell, the magnetic flux density B and the magnetic field H inside a core are related as

$$B = \mu_0\mu_r H\,, \tag{3}$$

where μ_r represents the relative permeability, which varies depending on the spin alignment within the core; factors such as the core's length, thickness, and shape anisotropy are key determinants of this property. In other words, in the pre-saturation region, μ_r remains high, making it easier for the core to become magnetized by external fields. However, near the saturation point, where spins are maximally aligned, μ_r decreases sharply, making it difficult to further increase magnetization. Consequently, this leads to the aforementioned non-linear behavior and a reduction in the dynamic range.

Increasing the core thickness resulted in a low magnetic flux density within the core under the same external magnetic field conditions, requiring a significantly stronger magnetic field to reach saturation, thereby extending the dynamic range. However, because the changes in the magnetic flux density within the core became gradual, the sensitivity decreased.

To optimize the OFG sensor, we evaluated the sensitivity and dynamic range based on the core shape by setting the core length

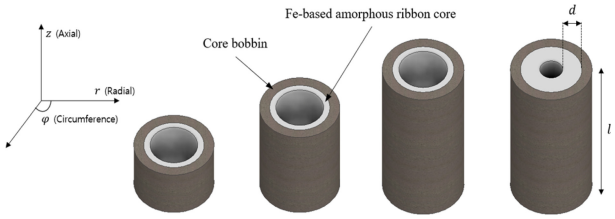

Fig. 6. Optimization parameter of OFG sensor

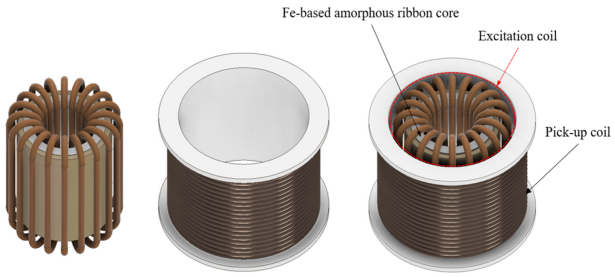

Fig. 7. Optimized design of OFG sensor

(l) and thickness (d) as parameters as shown in Fig. 6. The core length (l) was set to 2 mm, 4 mm, and 6 mm, and the thickness (d) was set to 50 μm and 150 μm. The ferromagnetic core was constructed using an Fe-based amorphous ribbon. As shown in Fig. 7, the excitation coil was 120-μm copper wire with 20 turns wound in the z-direction around the configured core, and the pickup coil was 50-μm copper wire with 500 turns wound in the Φ-direction.

4. EXPERIMENTAL RESULT

4.1 Experimental Results of OFG Sensor

Fig. 8 shows a block diagram of the setup designed to measure the output changes in the OFG sensor in response to external magnetic fields. Alternating current from a function generator was applied to the excitation coil to magnetize the core. Simultaneously, a uniform DC magnetic field was applied through a Helmholtz coil, and the output voltage signal obtained via an oscilloscope was monitored.

Fig. 9 (a) shows the changes in the output voltage according to the core length when an external magnetic field was applied. When the core length was 2 mm, the sensitivity was extremely low at 213 V/T. Although its dynamic range was wide, it was difficult to obtain sufficiently large output signals. When the core length was 4 mm, the sensitivity increased to 5,040 V/T, and at 6 mm it reached 7,390 V/T owing to the rapid saturation.

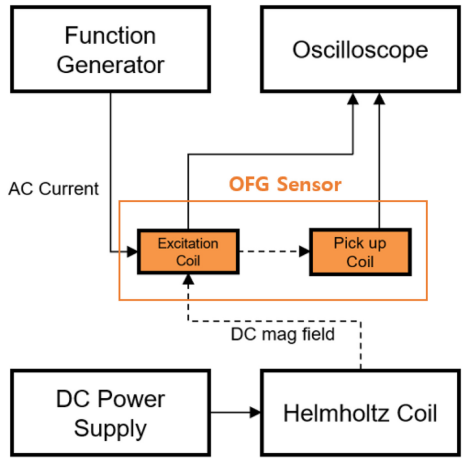

Fig. 8. Block diagram of setup for OFG sensor properties test

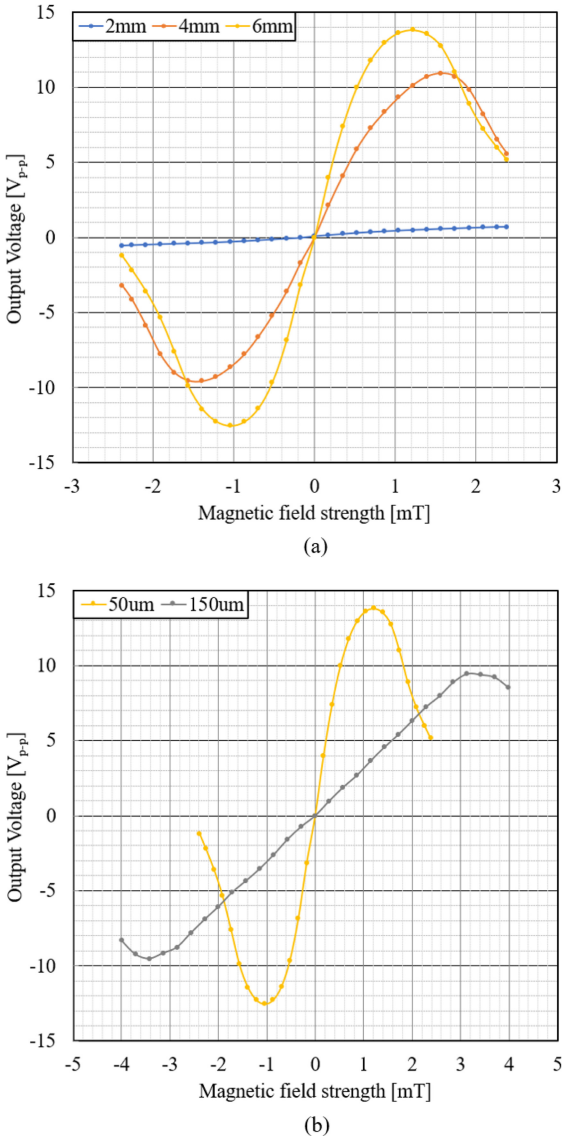

Fig. 9. Measurement results of OFG sensor properties : (a) core length and (b) core thickness

However, the dynamic range narrowed to ±1.5 mT at 4 mm and ±1 mT at 6 mm.

To further validate these findings, the sensor sensitivity S was quantified using the relationship

$$S \approx \frac{\partial V_{out}}{\partial B_{ext}}, \tag{4}$$

where V_{out} is the output voltage measured at the pickup coil and B_{ext} is the external magnetic field applied. A higher S value indicates a steeper slope of the V_{out} versus B_{ext} curve, implying that the sensor can detect slight changes in the magnetic field more effectively. In this context, the dynamic range DR may be defined as the field range over which the sensor output maintains a sufficiently linear or stable response.

One way to approximate the DR is to identify the onset of saturation, H_{sat}, and use a proportional measure such as

$$DR \propto \mu_0 H_{sat}. \tag{5}$$

Increasing the core length accelerates the approach to saturation, thus boosting S but narrowing the DR. In contrast, shorter cores delay saturation, resulting in a wider DR but lower sensitivity. These trends highlight the tradeoff between sensitivity and dynamic range dictated primarily by the ability of the core to reach saturation.

Fig. 9 (b) shows the changes in the output voltage based on the core thickness when an external magnetic field was applied. When the core thickness was 50 μm, the sensitivity was 7,390 V/T. When the core thickness was increased to 150 μm, the sensitivity decreased to 3,130 V/T. However, a larger thickness allowed the core to accommodate more magnetic field before reaching saturation, thereby extending the dynamic range from ±1 mT to ±3.5 mT.

The experimental results confirmed that, as the core length increased, the sensitivity increased, whereas the dynamic range narrowed. In addition, as the core thickness increased, the sensitivity decreased, but the dynamic range expanded. An OFG sensor with high sensitivity and a dynamic range of ±3 mT or higher, suitable for the MFL magnetic environment was optimized. Our developed OFG sensor with a 6-mm core length and 150-μm core thickness achieved a dynamic range of ±3.5 mT and a high sensitivity of 3,130 V/T.

4.2 Experimental Results of MFL testing

In this study, we applied an optimized OFG sensor to an MFL magnetic environment to verify defect detection. Fig. 10 shows the MFL test results for each type of pipe defect in a 3D graph. The x-axis represents the time, the y-axis represents the output voltage, and the z-axis represents the changes in the DC magnetic field intensity applied to the pipe.

To quantitatively link the leakage flux to the applied DC flux, the total magnetic flux in the vicinity of the defect can be modeled as

$$B_{total} = B_{DC} + B_{leak}, \tag{6}$$

where B_{DC} is the uniformly applied DC magnetic field and B_{leak} represents the localized flux disturbance caused by the defect. From Maxwell's equations, particularly $\nabla \cdot B = 0$ and $\nabla \times H = J$, any discontinuity in the material alters the local permeability, causing the magnetic field lines to redistribute and form leakage flux.

As shown in Fig. 10 (a), because of the large defect depth, the leaked magnetic field detected by the sensor distinctly increased. When the DC magnetic field intensity was varied stepwise, defect detection became clearer. In Fig. 10 (b), defect identification was possible; however, the range of change in the leaked magnetic field was small owing to the small defect size.

As shown in Fig. 10 (c), as the magnetic field leakage occurred at the external surface of the pipe, distinct defect detection was confirmed, and as shown in Fig. 10 (d), defect identification was also possible. However, a shallow defect depth resulted in a lesser-leaked magnetic field and a more gradual change in the output voltage.

This study confirmed that the leaked magnetic field was clearly measured as the DC magnetic field intensity applied to the pipe gradually increased. This proves that the dynamic range and high sensitivity of the OFG sensor can be employed in MFL magnetic environments.

5. CONCLUSION

We confirmed that a tradeoff exists between the sensitivity and dynamic range of an OFG sensor by adjusting its core length and thickness. We measured the dynamic range suitable for an MFL testing environment and designed and fabricated an appropriate OFG sensor.

As a result, we confirmed sensor properties with a ±3.5-mT dynamic range and a sensitivity of 3,130 V/T, and defect detection was verified when the OFG sensor was applied to MFL testing.

In future studies, we plan to explore a variety of core materials and coil configurations to further optimize the sensor design. We

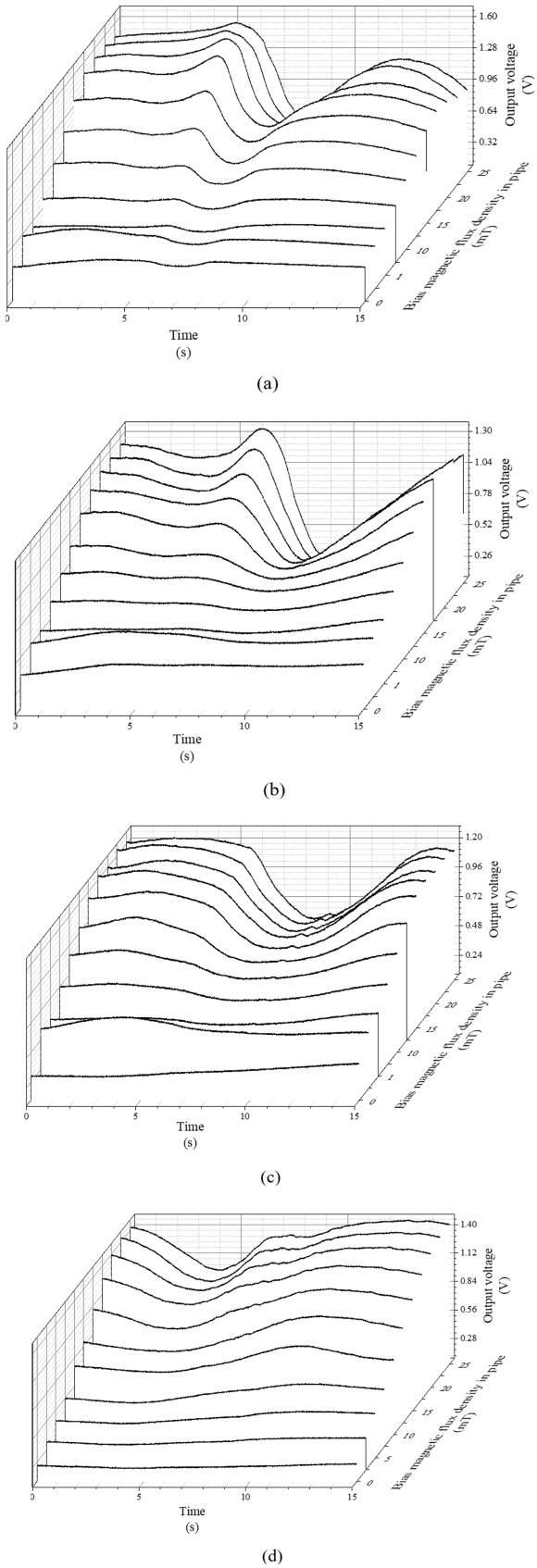

Fig. 10. Measurement results of MFL detector using OFG sensor : (a) 50% internal, (b) 10% internal, (c) 50% external, and (d) 10% external

will also pursue multicoil configurations that consider core thickness geometry and demagnetizing factors, aiming to maximize the sensitivity before reaching saturation while simultaneously expanding the dynamic range.

By improving the sensitivity of the sensors used for MFL, it is possible to detect defects at preliminary stages, such as initial corrosion or microcracks, contributing to pipeline maintenance and accident prevention.

ACKNOWLEDGMENT

This study was supported by the K-Sensor Technology Development Project of the Ministry of Trade, Industry, and Energy of the Republic of Korea [Project No.:RS-2022-00154902].

REFERENCES

[1] L. Zhang, Y. Bian, P. Jiang, Y. Huang, and Y. Liu, “Improving Pipeline Magnetic Flux Leakage (MFL) Detection Performance with Mixed Attention Mechnisms (AMs) and Deep Residual Shrinkage Networks (DRSNs)”, *IEEE Sens. J.*, Vol. 24, No. 4, 2024.

[2] H. Iqbal, S. Tesfamariam, H. Haider, and R. Sadiq, “Inspection and maintenance of oil & gas pipeline: A review of policies”, *Struct. Infrastruct. Eng.*, Vol. 13, No. 6, pp. 794-815, 2017.

[3] E. T. Ibrahim, C. Yang, G. Tian, M. Robinson, Q. Ma, and L. U. Daura, “Pulsed Magnetic Flux Leakage Measurement Using Magnetic Head and Tunneling Magnetoresistance for Defect Detection”, *IEEE Sens. J.*, Vol. 23, No. 17, pp. 19184-19193, 2023.

[4] Y. Shi, C. Zhang, R. Li, M. Cai, and G. Jia “Theory and application of magnetic flux leakage pipeline detection”, *Sens.*, Vol. 15, No. 12, pp. 31036-31055, 2015.

[5] H. Q. Pham, B. V. Tran, D. T. Doan, Q. N. Pham, K. Kim, C. Kim, F. Terki, and Q. H. Tran, “Highly Sensitive Planar Hall Magnetoresistive Sensor for Magnetic Flux Leakage Pipeline Inspection”, *IEEE Trans. Magn.*, Vol. 54, No. 6, pp. 1-5, 2018.

[6] D. Jiao, B. Gao, G. Ru, Q. Ma, J. Lei, Y. Zhang, J. F. Lu, and W. L. Woo, “Instrumentation of Cross Electromagnetic Eddy Current Sensing for Internal Pipeline Inspection”, *IEEE Sens. J.*, Vol. 24, No. 14, pp. 22745-22757, 2024.

[7] F. Yuan, Y. Yu, L. Li, and G. Tian, “Investigation of DC Electromagnetic-Based Motion Induced Eddy Current on NDT for Crack Detection”, *IEEE Sens. J.*, Vol. 21, No. 6, 2021.

[8] W. Gao, D. Zhang, and E. Zhang, “Defect Detection in the Dead Zone of Magnetostrictive Sensor for Pipe Monitoring”, *IEEE Sens. J.*, Vol. 21, No. 3, pp. 3420-3428, 2021.

[9] P. Gao, H. Geng, L. Yang, F. Zheng, and Y. Su, “Research on Quantification Method of Ellipsoidal Defects Based on

Leakage Magnetic Detection", *IEEE Sens. J.*, Vol. 24, No. 9, pp. 14503-14518, 2024.

[10] S. M. Dutta, F. H. Ghorbel, and R. K. Stanley, "Dipole modeling of magnetic flux leakage", *IEEE Trans. Magn.*, Vol. 45, No. 4, pp. 1959-1965, 2009.

[11] Q. Tang, B. Gao, G. Ru, G. Qin, W. L. Woo, S. Jiang, D. Chen, J. Li, and J. Cheng, "Physical Coupling Fusion Sensing of MFL-EMAT for Synchronous Surface and Internal Defects Inspection", *IEEE Sens. J.*, Vol. 23, No. 14, pp. 16068-16079, 2023.

[12] N. Murata and A. Matsuoka, "Practical Method for Drastic Improvement of Output Offset Stability in Bias-Switched Fundamental Mode Orthogonal Fluxgate", *IEEE Sens. J.*, Vol. 21, No. 17, pp. 18641-18649, 2021.

[13] N. Murata, H. Karo, I. Sasada, and T. Shimizu, "Fundamental mode orthogonal fluxgate magnetometer applicable for measurements of DC and low-frequency magnetic fields", *IEEE Sens. J.*, Vol. 18, No. 7, pp. 2705-2712, 2018.

[14] M. Butta, *"Orthogonal fluxgate magnetometers", in Smart Sensors, Measurement and Instrumentation*, S. C. Mukhopadhyay, Eds. Springer, Berlin, pp. 63-102, 2016.

[15] W. Y. Choi, J. S. Hwang, and S. O. Choi, "Micro fluxgate magnetic sensor using multi-layer PCB process", *J. Sen. Sci. Technol.*, Vol. 12, No. 2, pp.72-78, 2003.

[16] I. Sasada, "Orthogonal fluxgate mechanism operated with dc biased excitation", *J. Appl. Phys.*, Vol. 91, No. 10, pp. 7789-7791, 2002.